CONF-781053--2

PREPRINT UCRL-81473

Lawrence Livermore Laboratory

TIME-RESOLVED SUPRATHERMAL X-RAYS

Peter H. Y. Lee and Mordy D. Rosen

MASTER

August 30, 1978

This paper was prepared for submission to the APS Plasma Physics Meeting of the American Physical Society, Colorado Springs, Colorado, October 30-November 3, 1978.

This is a preprint of a paper intended for publication in a journal or proceedings. Since changes may be made before publication, this preprint is made available with the understanding that it will not be cited or reproduced without the permission of the author.

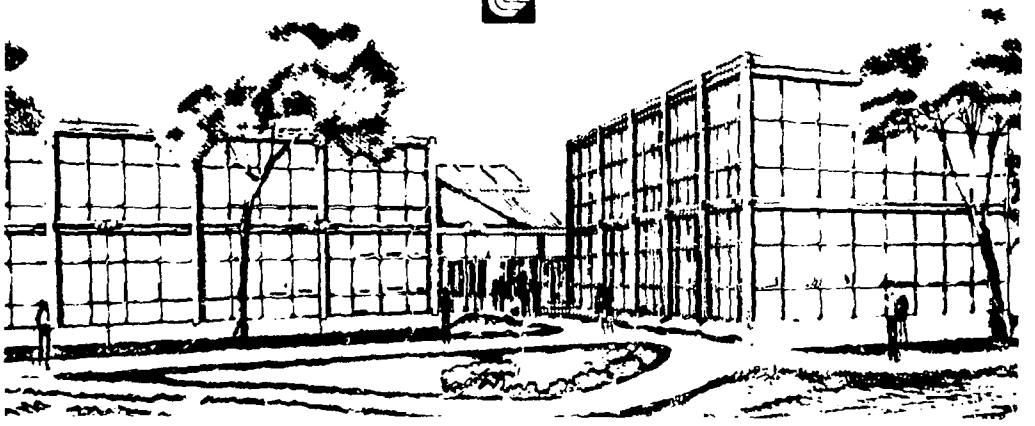

DISTRIBUTION OF THIS DOCUMENT IS UNLIMITED

NOTICE
This report was prepared as an account of work sponsored by the United States Government. Neither the United States nor the United States Department of Energy, nor any of their employees, nor any of their contractors, subcontractors, or their employees, makes any warranty, express or implied, or assumes any legal liability or responsibility for the accuracy, completeness or usefulness of any information, apparatus, product or process disclosed, or represents that its use would not infringe privately owned rights.

TIME RESOLVED SUPRATHERMAL X-RAYS

P. H. Y. Lee and M. D. Rosen

University of California Lawrence Livermore Laboratory
Livermore, California 94550

ABSTRACT

Temporally resolved x-ray spectra in the range of 1-20 keV have been obtained from gold disk targets irradiated by 1.06 μm laser pulses from the Argus facility. The x-ray streak camera used for the measurement has been calibrated for streak speed and dynamic range by using an air-gap Fabry-Perot etalon, and the instrument response has been calibrated using a multi-range monoenergetic x-ray source. The experimental results indicate that we are able to observe the "hot" x-ray temperature evolve in time and that the experimentally observed values can be qualitatively predicted by LASNEX code computations when the inhibited transport model is used.

---

* Work performed under the auspices of the U.S. Department of Energy, Contract Number W-7405-ENG-48.

DISTRIBUTION OF THIS DOCUMENT IS UNLIMITED

TIME-RESOLVED SUPRATHERMAL X-RAYS*

P. H. Y. Lee and M. D. Rosen

University of California, Lawrence Livermore Laboratory
Livermore, California 94550

In laser-produced plasmas, most of the electromagnetic radiation that the plasma emits is in the soft x-ray regime. The x-rays generated from bremsstrahlung and recombination radiation yield direct information on the electron temperature. On the other hand, suprathermal or "hot" electrons are generated by the resonance absorption mechanism[1-3] as well as other collective phenomena such as parametric decay and oscillating two-stream instabilities[4-7]. Time-integrated "hot" x-ray emissions arising from the nonthermal high energy tail on the electron energy distribution have been observed in laser-plasma interaction experiments[8,9]. For ablatively driven laser fusion targets, calculations show that suprathermal electrons generated by plasma instabilities tend to preheat the fuel and thus have a detrimental effect on target performance[10]. It is, therefore, important to study the temporal behavior

---

*Work performed under the auspices of the U. S. Department of Energy by Lawrence Livermore Laboratory under Contract No. W-7405-Eng-48.

of x-ray emission spectra of laser-produced plasmas for a better understanding of laser-plasma interactions and fusion target performance. In this paper we present the first temporally resolved x-ray emission spectra from laser-irradiated high-Z targets, which show the evolution of both thermal and hot x-rays in time.

The experiments were performed at 1.06 μm wavelength with one beam of the Argus laser facility[11], operating in this case with 250-350 J, 200-400 ps FWHM pulses, the typical intensity on target being in the 1-3 x 10^{15} W/cm^2 range. The targets consisted of gold disks, 300 μm in diameter and thicknesses between 10 - 50 μm. The instrument used for time resolved x-ray measurements is the Livermore 15 ps x-ray streak camera, which is described elsewhere[12]. For the present purpose, an 11-channel, K-edge filter pack was used. This is shown in Figure 1. The foil materials of this filter pack consisted of two channel thicknesses of polyvinylchloride (chlorine, K-edge at 2.8 keV), two of titanium (5 keV), two of cobalt (7.7 keV), one of zinc (9.7 keV), one of yttrium (17 keV), two of molybdenum (20 keV) and one of silver (25.5 keV). Appropriate foil thicknesses of the respective channels were chosen to provide optimum channel responses and double channels of varying thicknesses were used to accomodate the large dynamic range in emission intensities and to provide for error bar estimates in given spectral regions.

The instrument response of the x-ray streak camera was calibrated at a multi-range monoenergetic x-ray source from 4.5 to 98 keV. The instrument streak speed and dynamic range were calibrated on a small one-Joule laser facility by using an air-gap Fabry - Perot etalon with reflectivities of 50% and ~100%. A typical streak record is shown in Figure 2. The x-rays were generated by a train of 1.06 μm pulses, of monotonically decreasing intensity and separated by the double transit-time of the etalon, incident upon an

aluminum target. The corresponding calibrated microdensitometer trace of the streak record is also shown in this figure. Note that the dynamic range in this case is three orders of magnitude.

From the streak records, one obtains the time-resolved x-ray emissions for each channel by using the measured instrument streak speed. By using the measured instrument response, the x-ray intensities of the different channels can be related to one another in relative intensity and provide an unfold of the x-ray emission spectra at any given time during the laser interaction with the target.

We note that the hot x-rays, i.e., emissions at energy channels higher than ~10 keV, have a temporal behavior which essentially follows the laser pulse. This manifestation is especially evident for 200 ps FWHM shots with laser intensities in the 3 x 10^{15} W/cm^2 range[13]. This is the first time-resolved direct observation of the long suspected suprathermal x-ray behavior due to hot electrons produced by collective (resonant or parametric) processes. In addition, at high laser intensities the thermal temperature of the hot underdense corona can reach many keV. For example, setting the absorbed intensity equal to $fn_{cr}v_eT_e$ where f is the flux inhibitor, n_{cr} the critical density, v_e and T_e the electron thermal velocity and temperature, respectively, then for I = 3 x 10^{15} W/cm^2, and assuming 20% absorption, T_e = 2 keV for f = 1 and T_e = 10 keV for f = 0.1.

A sample set of time-resolved high energy x-ray spectra is shown in Figure 3 for a 300 μm-diameter, 10 μm-thick gold disk target. The target was irradiated by a 330 J, 400 ps (FWHM) pulse. The peak intensity for this experiment was 1.7 x 10^{15} W/cm^2, the measured absorption was 20%. The time scale is chosen such that zero time refers to the time when all 11 channels have peak emission. From this figure, one can clearly see the evolution of the high-

energy tail slope in time. The suprathermal or hot x-ray temperature, θ_H, is defined by the slope of the spectrum in the energy range above ~8 keV. The high energy tail is being detected at about 180 ps before peak x-ray emission, gradually increasing to a maximum θ_H value of 9 keV at the peak, and then decreasing with diminishing laser power. It is also apparent from the spectra that the thermal x-ray temperature, θ_c, defined by the slope of the spectrum in the energy range below ~8 keV, is decoupled from the hot x-ray temperature throughout the laser pulse, having a fairly constant value of about 0.7 to 0.8 keV. It should be noted that the presence of prominent gold spectral lines at around 2.5 keV makes the determination of θ_c somewhat less accurate.

A comparison of the experimental results with LASNEX[14] code predictions is shown in Figures 4 and 5 for both the hot and thermal x-ray temperatures, respectively. The LASNEX computation is made under the assumption that inverse bremsstrahlung is the principal absorption mechanism and about 20% of the remaining light that reaches the critical surface is reasonantly absorbed, creating an electron distribution, characterized by a T_H given by

$$T_H = T_B + 49.4\ (I\lambda^2)^{0.425}\ T_B^{0.4} \left(1 + \frac{3T_i}{ZT_B}\right)^{0.25}, \qquad (1)$$

where T_B is the average electron temperature in keV, T_i is the ion temperature, I is the laser intensity in units of 10^{17} W/cm^2, λ is the incident laser wavelengths in microns, Z is the charge state of the target material at critical density and T_H is the hot electron temperature. Note that T_H is not the same as θ_H; θ_H is defined operationally by the slope of the code-produced x-ray spectra generated by the electrons. Equation (1) is based on particle simulations[3,15]. For the case where the heat flux is inhibited by ion-acoustic turbulence, thought to readily occur in high-Z plasmas[16],

there is qualitative agreement between code predictions and experiment (see Figure 4, inhibited transport curve), the code predicting somewhat higher values before and after the peak of the pulse, however, the value of θ_H at peak emission is predicted accurately to within 10% of the measurement. On the other hand, if the heat flux is not inhibited, the plasma corona is cooled, thereby increasing the inverse bremsstrahlung, and only 10% of the incident laser light ends up as being resonantly absorbed. The non-inhibited transport curve in Figure 4 clearly shows that such a mix of absorptions does not match the observed data. Also plotted in Figure 4 is the laser pulse normalized by its peak value. Although we have no time fiducial, we have chosen to match the peak of the laser pulse with the peak of the x-ray emission pulse. This seems reasonable in terms of the resonance absorption theory[1-3]; since θ_c is roughly constant, the ratio of the electron quiver velocity to the thermal velocity is maximum at the peak of the laser pulse (for θ_c = 0.7 keV and I = 1.7 x 10^{15} W/cm^2, $v_{osc}/v_{th} \sim 1$). Consequently, the highest energy electrons are generated at that time and therefore the x-rays should be the hottest. We note that if θ_H scales like I^n, then the measured data indicate that $n \simeq 1$ before the peak and $n \gtrsim 1$ after the peak, whereas the code using the inhibited transport model suggests that $n < 1$ before the peak and $n \lesssim 1$ after the peak. A likely explanation for n being different before and after the peak is that the plasma density profile and corona evolve in time and thus are asymmetric with respect to the peak of the laser pulse. Earlier experimental and theoretical analyses[2,3] of θ_H which suggested $n \approx 1/3$, were based on time-integrated data, and thus reflect θ_H vs. I (peak value) behavior only. Our own measurement of the peak time-resolved θ_H indeed matches those earlier predictions, but throughout the pulse, n is clearly much greater than 1/3. From a target design point of

view, since most of the preheating electrons are created near the peak of the pulse, it is only there that a predictive capability is essential, and thus the earlier analyses are still quite relevant. From a basic physics point of view, however, this difference in n requires further study and understanding.

The code predictions for the thermal x-ray temperature yield values which are slightly lower than the measured values (see Figure 5), but again, we emphasize that the major feature is in good agreement with the experiment, namely, θ_C is fairly constant throughout the laser pulse, while θ_H is not. This fact suggests that the behavior of the thermal electrons are governed by conventional processes such as hydrodynamics and thermal conduction, while the suprathermal electrons follow the short laser pulse time scale when collective processes are effective.

Independent measurements on this particular experiment with a different diagnostic yield time-integrated data[17] of $\theta_C = 0.7 \pm 0.15$ keV and $\theta_H = 14.1 \pm 3$ keV which are in reasonable agreement with the x-ray streak camera data as well as the code predictions.

In conclusion, we have succeeded in obtaining time-resolved high energy x-ray spectra by using an x-ray streak camera with multi-channel filter packs. The results are such that we are able to observe both the thermal and suprathermal x-ray temperature evolve in time. We observed that while θ_H follows the laser pulse on grounds explainable by collective plasma processes, θ_C remains fairly constant and decoupled from θ_H suggesting some sort of inhibition mechanism at work.

We are especially indebted to D. T. Attwood for many helpful and stimulating discussions. The authors acknowledge the material support and encouragement of their many colleagues in the Livermore Laser Fusion Program, in particular, K. G. Estabrook, H. N. Kornblum, E. L. Pierce, M. J. Boyle, E. M. Campbell, H. G. Ahlstrom, and E. K. Storm.

References

1. K. G. Estabrook E. J. Valeo, and W. L. Kruer, Phys Fluids 18, 1151 (1975).

2. D. W. Forslund, J. M. Kindel, and K. Lee, Phys. Rev. Lett. 39, 284 (1977).

3. K. Estabrook and W. L. Kruer, Phys. Rev. Lett. 40, 42 (1978).

4. K. Mizuno and J. S. DeGroot, Phys. Rev. Lett. 35, 219 (1975).

5. J. Denavit, Phys. Fluids 19, 972 (1976).

6. W. L. Kruer and J. M. Dawson, Phys. Fluids 15, 446 (1972).

7. J. I. Katz et al, Phys. Fluids 16, 1519 (1973).

8. R. A. Haas et al, Phys. Fluids 20, 322 (1977).

9. E. K. Storm et al, Phys. Rev. Lett. 40, 1570 (1978).

10. J. Nuckolls et al, Nature 239, 139 (1972).

11. W. W. Simmons et al, Appl. Optics 17, 999 (1978).

12. D. T. Attwood et al, Phys. Rev. Lett. 37, 499 (1976).

13. P. H. Y. Lee et al, Bull. Am. Phys. Soc. 22, 1113 (1977).

14. G. B. Zimmerman, Lawrence Livermore Laboratory Rept. No. UCRL-76927, (1975) Unpublished.

15. K. G. Estabrook, private communications.

16. M. D. Rosen et al, "High-Z Disc Experiments" Laser Program Annual Report - 1977, Lawrence Livermore Laboratory (to appear).

17. H. N. Kornblum, private communications.

Reference to a company or product name does not imply approval or recommendation of the product by the University of California or the U.S. Department of Energy to the exclusion of others that may be suitable.

NOTICE

"This report was prepared as an account of work sponsored by the United States Government. Neither the United States nor the United States Department of Energy, nor any of their employees, nor any of their contractors, subcontractors, or their employees, makes any warranty, express or implied, or assumes any legal liability or responsibility for the accuracy, completeness or usefulness of any information, apparatus, product or process disclosed, or represents that its use would not infringe privately-owned rights."

Fig. 1 THE 11-CHANNEL FILTER PACK

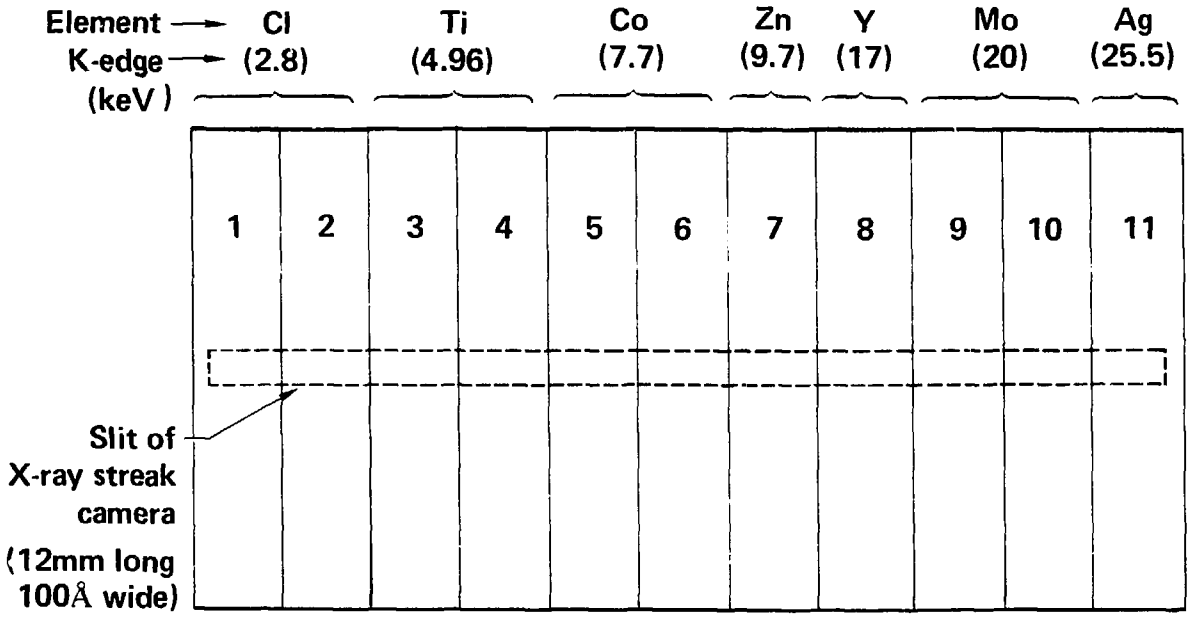

20-50-0878-2710

Fig. 2 **A STREAK RECORD AND THE CORRESPONDING CALIBRATED MIRODENSITOMETER TRACE USED FOR INSTRUMENT SWEEP SPEED AND DYNAMIC RANGE CALIBRATION**

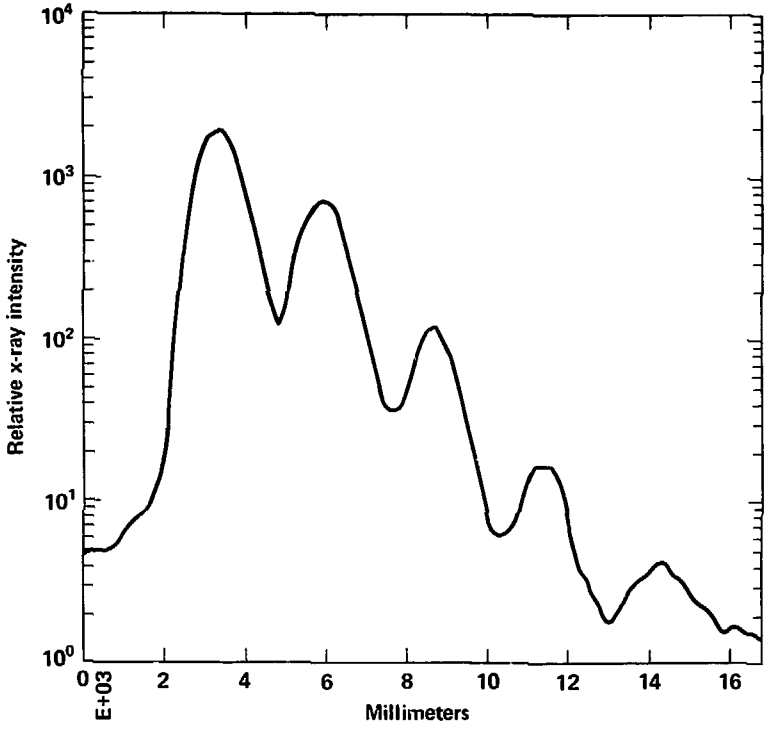

20-50-0878-2711

Fig. 3 **TIME RESOLVED X-RAY SPECTRA OF 1.06 μm LASER-IRRADIATED Au-DISK (332J/400 ps, 1.69 $\times$ 10^{15} W/cm^2)**

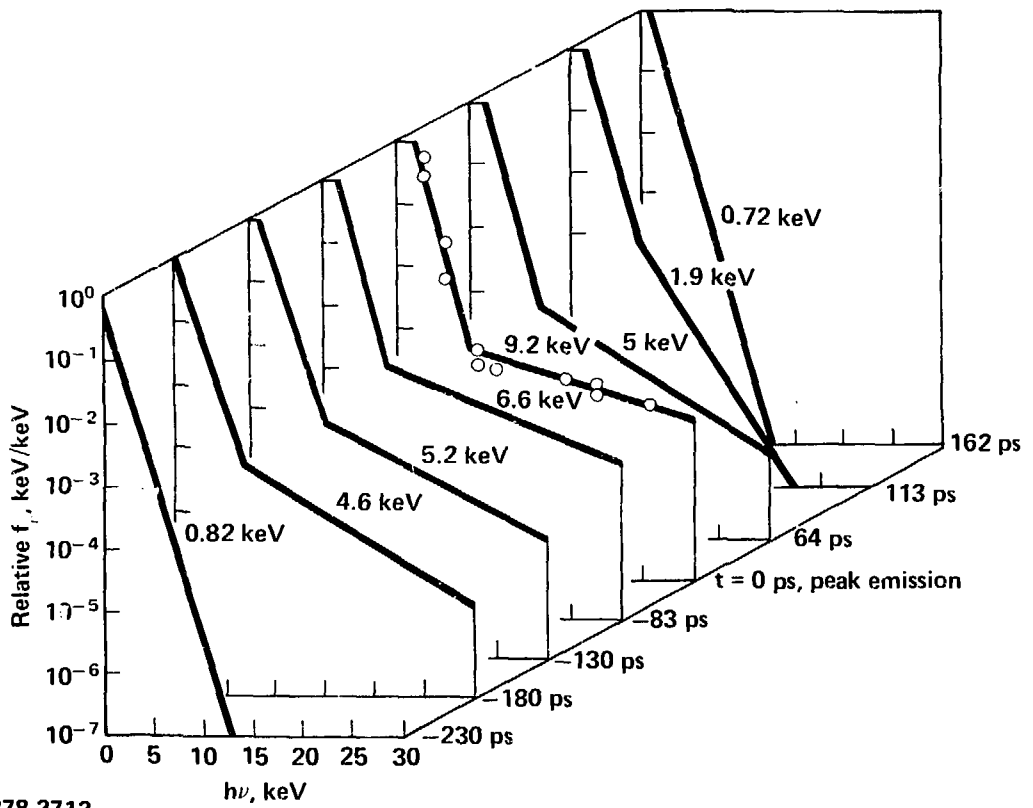

20-50-0878-2712

Fig. 4

COMPARISON OF MEASURED AND LASNEX CODE PREDICTED "HOT" X-RAY TEMPERATURES FOR 400 ps FWHM LASER PLUSE

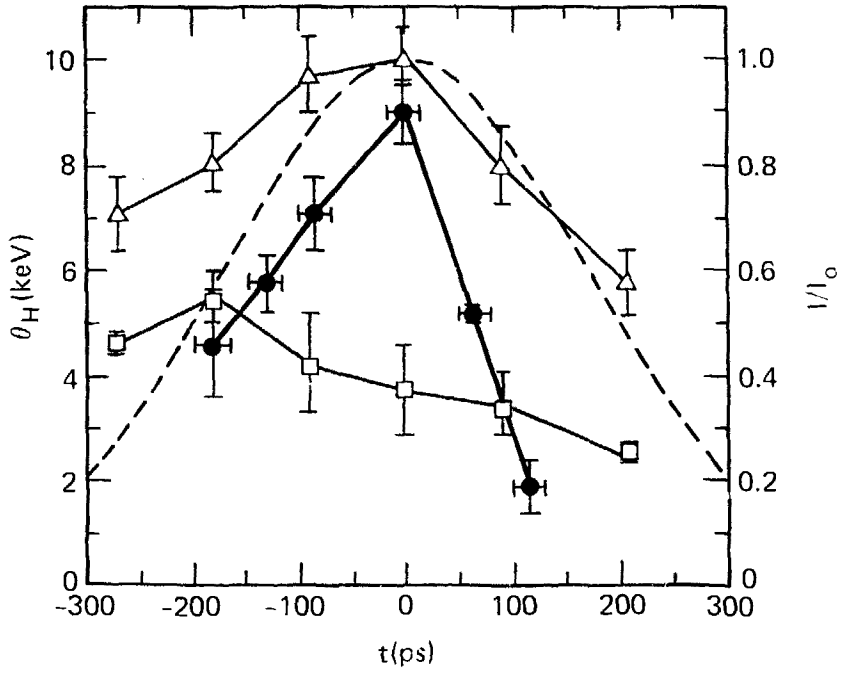

● Experiment
△ Lasnex (inhibited transport)
----Laser pulse
□ Lasnex (non-inhibited transport)

20-50-0878-3012

Fig. 5

COMPARISON OF MEASURED AND LASNEX CODE PREDICTED "COLD" X-RAY TEMPERATURES

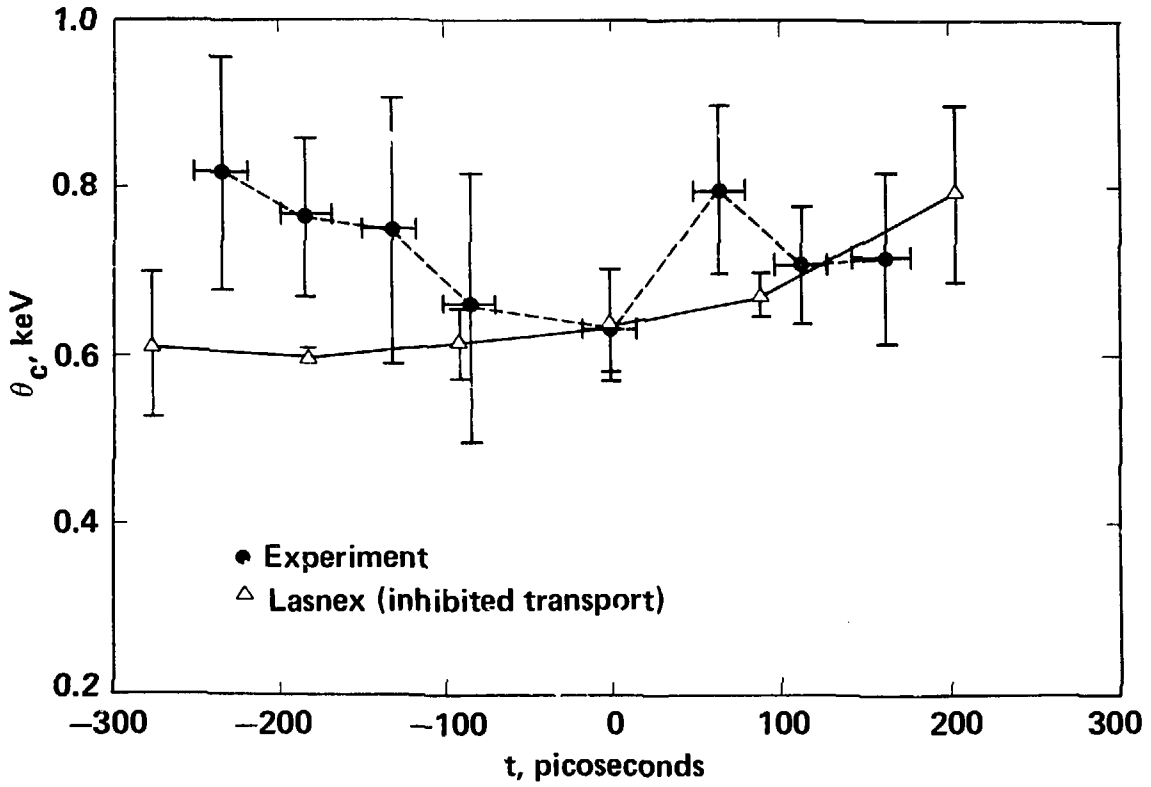

20-50-0878-2714